Hamburger Beiträge
zur Angewandten Mathematik

Image Processing for Numerical Approximations of Conservation Laws: Nonlinear anisotropic artificial dissipation

Thorsten Grahs, Andreas Meister, Thomas Sonar

Reihe F
Computational Fluid Dynamics and Data Analysis 8
December 1998

Hamburger Beiträge zur Angewandten Mathematik

Reihe A	Preprints
Reihe B	Berichte
Reihe C	Mathematische Modelle und Simulation
Reihe D	Elektrische Netzwerke und Bauelemente
Reihe E	Scientific Computing
Reihe F	Computational Fluid Dynamics and Data Analysis

Image Processing for Numerical Approximations of Conservation Laws: Nonlinear anisotropic artificial dissipation

Thorsten Grahs, Andreas Meister
Thomas Sonar
Institut für Angewandte Mathematik
Universität Hamburg
Bundesstraße 55, D-20146 Hamburg
sonar@math.uni-hamburg.de

December 22, 1998

Abstract We employ a nonlinear anisotropic diffusion operator like the ones used as a means of filtering and edge enhancement in image processing, in numerical methods for conservation laws. It turns out that algorithms currently used in image processing are very well suited for the design of nonlinear higher-order dissipative terms. In particular, we stabilize the well-known Lax-Wendroff formula by means of a nonlinear diffusion term.

1 Introduction

The construction of suitable artificial viscosity terms for stabilizing finite difference schemes of higher order is a difficult task. In the last decade we observed therefore a strong tendency to construct numerical approximations of conservation laws without explicit knowledge of their numerical diffusion. The modern total variation diminishing (TVD) or essentially non-oscillatory (ENO) schemes belong to this class, in which a basic first-order scheme is enhanced by the use of sophisticated recovery functions, see [8], [3]. There are, however, certain circumstances in which an approach using explicit construction of artificial dissipation would be advantageous. If we consider pseudospectral methods the concept of ENO recovery is very

hard to apply if the degree of the basis polynomials used is high. Here one would like to compute shocked solutions with central differences and to post-process the oscillatory numerical solution such that

- high frequency oscillations are filtered, and
- shocks are steepened and represented with high resolution.

Another area of application is gridfree methods, see [1], where modern concepts of recovery fail due to the irregularity of the interpolation points. In that case one would like to compute all derivatives from a central interpolant (or, better, a least squares approximation) and post-process the derivatives as was described above.

Over the years there were no general attempts to derive a constructive theory which would enable the design of suitable artificial viscosities within the CFD community. However, filtering and edge enhancement is a fundamental task in image processing and in recent years a theory of nonlinear anisotropic diffusion was created and can now be found in textbooks like [12] and [4]. In a noisy picture one also would like to filter the high freuqency components before detecting the edges (i.e. jumps in grey level). Then one would like to enhance the edges in order to represent the edges in high resolution. Now there is nothing which keeps us from interpreting our numerical solution corresponding to a conservation law as a photograph or picture, at least not in the case of steady solutions. In the same way the photographer would very much prefer to see the contours on his picture as sharp thin lines the numerical analyst would prefer to see shocks as crispy lines instead as smeared thick regions. To accomplish this picture as well as numerical solution have to be denoised. After removing the high frequencies we would like to spend a dose of diffusion tangential to shocks, but we would like to avoid diffusion across shocks (that is what anisotropy is all about). In contrast, in the vicinity of shocks we would like to solve a kind of nonlinear anisotropic backward heat equation to enhance the structure of a shock. Devices and algorithms satisfying exactly these requirements are ready to use if one is willing to enter the area of image processing.

The aim of this paper is mainly to show the potential of the methods developed for image processing if they are applied consistently to problems in the numerical treatment of hyperbolic conservation laws. We hope that we open up a new chapter in the design of modern nonlinear discretizations of conservation laws by using concepts which are well-known in the image processing society. In the present paper we demonstrate our algorithms with the Lax-Wendroff formula for two-dimensional scalar equations. A

future paper will be devoted to more serious applications in the field of gas dynamics.

The outline of the paper is as follows. After a brief review of the concepts used in the numerical treatment of conservation laws we apply the classical Lax-Wendroff formula to a steady nonlinear problem in which a shock is present. As is well-known the second-order Lax-Wendroff formula answers these type of problems with violent oscillations. In image processing Gaussian smoothing would be applied to the numerical solution in order to filter high frequency components. We exemplify this strategy but never use it in our final algorithms. On one hand the control of the linear diffusion is very difficult (a little overdose deteriorates the numerical solution strongly), on the other hand there are no visible differences in the final solution when computed with or without pre-smoothing. We then utilize the structure tensor which serves as a detector of the local coherence of our solution. In looking at eigenvalues and eigenvectors regions of anisotropy can be detected as well as regions of constant states. We then proceed to the construction of a nonlinear anisotropic artificial viscosity term. It is here where one has the freedom to choose between many different possible models. In our paper we decided to use an anisotropic regularization of the classical Perona-Malik model due to Weickert. There are certainly more clever choices but all the important ideas are contained in this specific example. This anisotropic artificial dissipation is discretized so that the discrete equation is stable. The underlying algorithm controlling the discretization is also taken from image processing. The final result reveals the post-processed Lax-Wendroff solution showing high-resolution of the shock and smooth behaviour in the continuous regions. Finally we construct a new splitting scheme containing the algorithmic ingredients described above.

The final algorithm may be displayed in form of the following flowchart.

- In every time step:

    1. Compute a numerical solution $U(t + \Delta t)$ with a finite difference method.
    2. If necessary, filter high frequency components by means of $U_\delta := K_\delta * U$, where K_δ is the Gaussian kernel corresponding to a standard deviation of δ.
    3. Compute the structure tensor $J_0(\nabla U_\delta)$ which contains information about the local coherence of the numerical solution.
    4. Average the structure information in the vicinity of each grid point in order to define a region size in which the orientation

of the solution is examined. This corresponds to computing $J_\rho(\nabla U_\delta) := K_\rho * J_0(\nabla U_\delta)$.

5. Construct an artificial dissipation D from knowledge contained in J_ρ.
6. Solve the discrete version of the nonlinear anisotropic equation

$$\begin{aligned} \partial_t w &= \text{div } (D(w)\text{grad } w) \\ w(x, y, 0) &= U_\delta(x, y) \end{aligned}$$

up to a user-defined pseudo-time τ.

- End of time step: Set $U(t + \Delta t) := w(\tau)$.

2 Conservation laws and finite difference schemes

Consider the scalar conservation law

$$\partial_t u + \partial_x f(u) + \partial_y g(u) = 0 \tag{1}$$

on $\Omega := [0, 1]^2$ where we assume Cauchy data $u_0(x, y) = u(x, y, 0)$ as well as boundary data which may respect the charasteristic directions. As is well known, discontinuities develop in general within finite time regardless how smooth the initial data is chosen.

We consider conservative three-point finite difference approximations

$$\begin{aligned} U_{i,j}^{n+1} = U_{i,j}^n &- \Delta t \frac{1}{\Delta x}\left[\Theta(U_{i+1,j}^n, U_{i,j}^n) - \Theta(U_{i,j}^n, U_{i-1,j}^n)\right] \\ &- \Delta t \frac{1}{\Delta y}\left[\Xi(U_{i,j+1}^n, U_{i,j}^n) - \Xi(U_{i,j}^n, U_{i,j-1}^n)\right] \end{aligned}$$

of (1) where Θ and Ξ denote numerical flux functions consistent in the sense of $\Theta(s, s) = f(s)$ and $\Xi(s, s) = g(s)$ for all $s \in \mathbf{R}$. It is well-known that every numerical flux of a three-point scheme can be written in the viscosity form

$$\Theta(v, w) := \frac{1}{2}(f(v) + f(w)) - \mathcal{Q}(v, w)(v - w),$$

where $\mathcal{Q}$ is the numerical viscosity coefficient, see [9].

It was shown by Tadmor in [9] and [10] that in the class of monotone – and, hence, first-order – schemes, there exists a minimax pair in the sense that a scheme with numerical viscosity coefficient $\mathcal{Q}$ which satisfies the inequality

$$\forall v, w \in S \subset \mathbf{R}: \quad \mathcal{Q}^G(v, w) \le \mathcal{Q}(v, w) \le \mathcal{Q}^{mLF}(v, w)$$

is entropy stable, i.e. converges to the entropy weak solution. Here S denotes the state space of possible values of the solution. It turns out that the minimax pair is given by two well known finite difference schemes, namely the Godunov scheme, corresponding to $\mathcal{Q}^{\mathrm{G}}$, and the (modified) Lax-Friedrichs scheme, corresponding to $\mathcal{Q}^{\mathrm{LF}}$. Both schemes are only first order accurate so that there is need for a constructive recipe giving higher order schemes from lower order ones.

In principle there are two different ways for the construction of higher order numerical methods. One could start directly with the construction of a numerical viscosity coefficient which gives higher order as well as stability. This is the way chosen by Jameson et al. in the early 1980's, see [2]. The construction is difficult due to the inherent nonlinearity of the problem and a well-behaving dissipation is hard to obtain. However, Jameson's codes still belong to the most successful pieces of software ever written and are known for their flexiblity as well as for their stability. The other route leading to stable higher order schemes developed into a mainstream in the mid 80's. Here one starts with a lower order monoton scheme, recovers the solution (with a MUSCL or ENO technique) and inserts the recovered solution into the low order flux functions. The recipe is quite general and the most spectactular finite difference schemes of our time, like the TVD or ENO schemes, rely on that construction. Although the process of recovery in itself is not an easy task we know now quite well how this can be done even on unstructured grids. In this class of methods we do not even see the numerical dissipation of our methods explicitly, which may seem a big advantage over the Jameson-type schemes.

However, in recent years a theory of nonlinear anisotropic diffusion was developed within the community of image processing. The algorithms developed there are very well suited for use in the numerical solution of conservation laws. In doing so, we proceed again along the lines of Jameson et al. and try to construct a reasonable dissipation coefficient directly, but we shall see that the algorithmic background is so well developed that we arrive safely at new nonlinear anisotropic dissipation terms, which turn the oscillating Lax-Wendroff scheme into a high resolution method.

3 The numerical solution viewed as a picture

It is well known that the Lax-Wendroff formula is a second-order finite difference scheme for (1). In two dimensions there are a variety of different

implementations but we have chosen the one described by Shokin [5], i.e.

$$\begin{aligned}
&\frac{U_{i,j}^{n+1}-U_{i,j}^{n}}{\Delta t}+\frac{F_{i+1,j}^{n}-F_{i-1,j}^{n}}{2\Delta x}+\frac{G_{i,j+1}^{n}-G_{i,j-1}^{n}}{2\Delta y}= \qquad (2)\\
&\frac{\kappa_x}{2}\left[A_{i+1/2,j}^{n}\left(\frac{F_{i+1,j}^{n}-F_{i,j}^{n}}{\Delta x}+\frac{G_{i+1/2,j+1/2}^{n}-G_{i+1/2,j-1/2}^{n}}{\Delta y}\right)\right.\\
&\left.-A_{i-1/2,j}^{n}\left(\frac{F_{i,j}^{n}-F_{i-1,j}^{n}}{\Delta x}+\frac{G_{i-1/2,j+1/2}^{n}-G_{i-1/2,j-1/2}^{n}}{\Delta y}\right)\right]\\
&+\frac{\kappa_y}{2}\left[B_{i,j+1/2}^{n}\left(\frac{F_{i+1/2,j+1/2}^{n}-F_{i-1/2,j+1/2}^{n}}{\Delta x}+\frac{G_{i,j+1}^{n}-G_{i,j}^{n}}{\Delta y}\right)\right.\\
&\left.-B_{i,j-1/2}^{n}\left(\frac{F_{i+1/2,j-1/2}^{n}-F_{i-1/2,j-1/2}^{n}}{\Delta x}+\frac{G_{i,j}^{n}-G_{i,j-1}^{n}}{\Delta y}\right)\right].
\end{aligned}$$

Here, $F_{i,j}^{n} := f(U_{i,j}^{n})$ and $A_{i\pm1/2,j}^{n} := (f'(U_{i\pm1,j}^{n}) + f'(U_{i,j}^{n}))/2$, $B_{i,j\pm1/2}^{n} := (g'(U_{i,j\pm1}^{n}) + g'(U_{i,j}^{n}))/2$, $G_{i\pm1/2,j\pm1/2}^{n} := (G_{i\pm1,j\pm1}^{n} + G_{i,j})/2$, et cetera. The grid coefficients are $\kappa_x := \Delta t/\Delta x$, $\kappa_y := \Delta t/\Delta y$.

If σ denotes the maximum value of A and B and if we assume $\Delta x = \Delta y =: h$, then the Lax-Wendroff scheme can be shown to be linearly stable under the somehow pessimistic CFL-condition

$$\frac{\Delta t}{h}\sigma \le \frac{1}{2\sqrt{2}}.$$

This was the condition which was implemented in all our test cases.

If we now apply the Lax-Wendroff scheme to the boundary value problem

$$u(x,y,0) = \begin{cases} 1.5 & ; \quad x = 0 \\ -2.5x + 1.5 & ; \quad y = 0 \\ -1.0 & ; \quad x = 1 \end{cases}$$

with 50×50 points and determine the boundary condition on the upper side of the unit square through simple extrapolation, then we get a steady solution as shown in figure 1. The true solution consists of a fan-like continuous wave which develops into a shock. A schematic view of it can be seen in figure 2. Since the true solution satisfies the steady equation

$$\partial_y u + \partial_x \frac{u^2}{2} = 0$$

the characteristic equations are given by $dy/ds = 1, dx/ds = u$, i.e.

$$\frac{dy}{dx} = \frac{1}{u}.$$

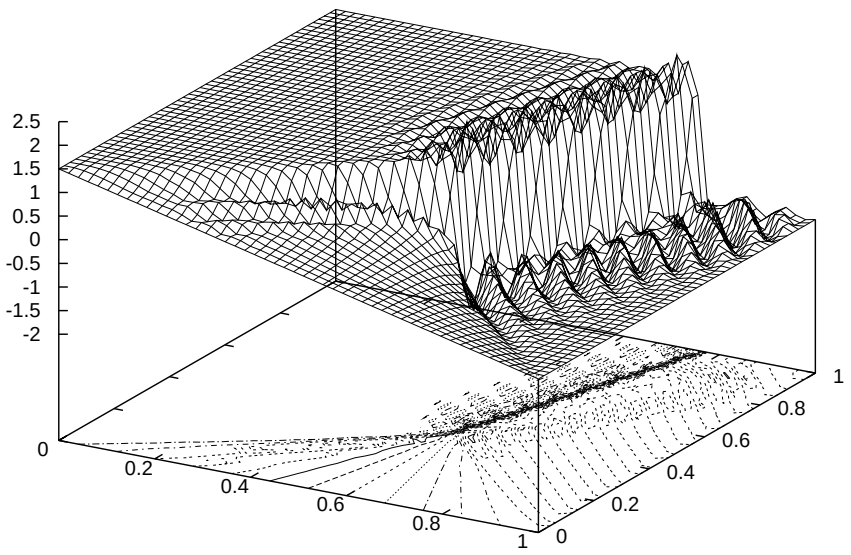

Figure 1: Lax-Wendroff solution of test problem

If we denote by u_L and u_R the given left and right state at $y = 0$, respectively, and we assume a linear distribution

$$u(x, 0) = (u_R - u_L)x + u_L$$

of the boundary data at $y = 0$, then the equation of the leftmost characteristic g_1 is given by $y = x/u_L$. The rightmost characteristic g_2 is given by $y = (x - 1)/u_R$. They meet at the point P where the shock g_3 starts. The coordinates of P are easily computed to be $x_P = u_L/(u_L - u_R)$ and $y_P = 1/(u_L - u_R)$. From the Rankine-Hugoniot condition we get for the shock g_3 the slope

$$\frac{dy}{dx} = \frac{2}{u_L + u_R}$$

and finally the equation $y = (2x - 1)/(u_L + u_R)$. From these equations it is easy to compute the true solution pointwise. If the solution is to be known at a point Q lying within the fan region than the characteristic connecting P and Q meets the x-axis at the point $x_{PQ} = x_P + y_p(x_Q - x_P)/(y_P - y_Q)$ which, according to our assumed linear boundary data distribution at $y = 0$, leads to $u_Q = (u_R - u_L)x_{PQ} + u_L$, which completes the description of the true solution.

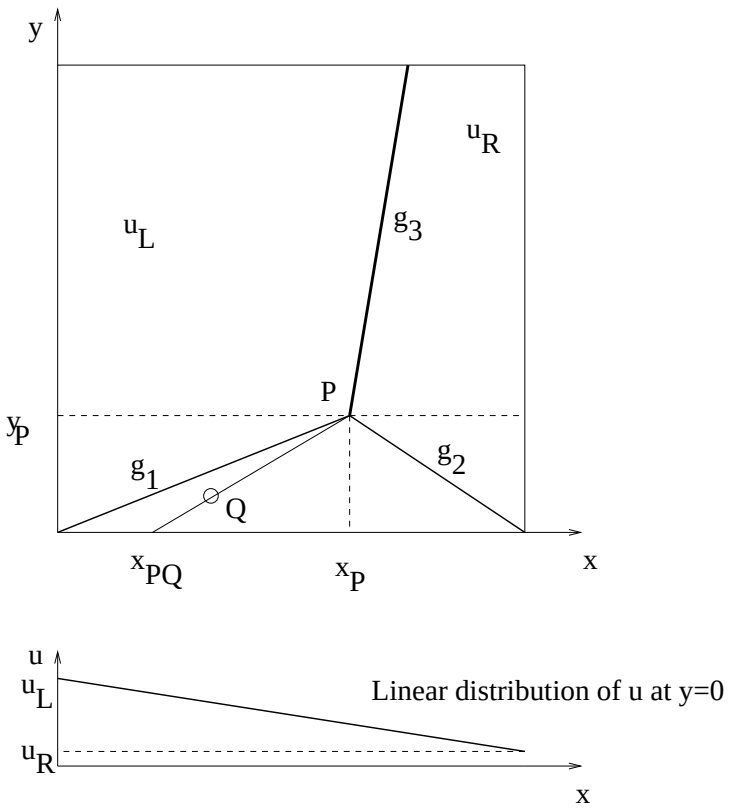

Figure 2: True solution of the model problem in (x, y) plane

In figure 3 we plotted the pointwise difference between the numerical and the true solution. As can be observed from the numerical solution there are strong oscillations present in the numerical solution; a behaviour which the Lax-Wendroff formula shares with other second-order schemes which do not respect monotonicity conditions. We are now going to correct these behaviour by means borrowed from image analysis.

If we look at the isolines we can think of them as being a photograph. The numerical solution as plotted above the isolines is then interpreted as the grey level function. Obviously, there is noise in the picture (the oscillating part) but there is also an edge (the shock) which is the main feature of the picture. We would now like to do two things, namely

1. enhance the edge, and

2. filter the oscillations.

In classical construction of artificial dissipation terms the fullfilment of both requirements leads into trouble. While a diffusion certainly filters the high

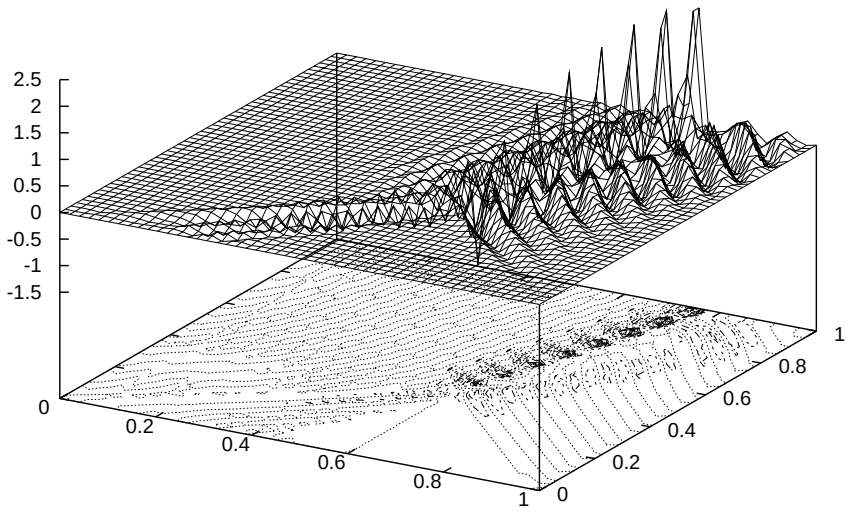

Figure 3: Difference between Lax-Wendroff solution and true solution

frequency oscillations it would also deteriorate the quality of the shock. In Jameson's dissipation model there is therefore a shock sensor, modelled by the second derivative of the pressure, which cuts the dissipation off across shocks.

However, one would like to introduce dissipation parallel to the edges, but avoid dissipation across edges. Dissipation models which satisfy exactly these requirements can be found in nonlinear anisotropic diffusion models from image processing.

4 Structure tensors and dissipation models

Edge enhancement is one of the classical problems in image processing. It was clear quite early in the history of this topic that edge detection without smoothing would lead to unexceptable results due to the noise, see [11]. Therefore, edge detection is only useful if appropriate smoothing is applied beforehand. To accomplish this task Gaussian smoothing may be

applied, i.e. the numerical solution U is convolved with the Gaussian kernel

$$U_\delta := K_\delta * U, \quad K_\delta(x,y) := \frac{1}{2\pi\delta^2}\exp\left(-\frac{x^2+y^2}{2\delta^2}\right).$$

The parameter δ is the width of the Gaussian. We do not intend, of course, to dive into a continuous scale-space theory like Weickert [12] or Morel and Solimini [4] in their respective books. In our framework we are given nothing but approximations of Dirac functionals $\langle \delta_{(x_i,y_j)}, u\rangle =: u_{i,j}$ at time $t = n\Delta t$ which we denote by $U^n_{i,j}$. Rearranging all those values (in lexicographical order, say), results in a vector $U := (U^n_{i,j})_{1\le i\le I, 1\le j\le J}$. Of course would it be possible to construct a smooth interpolant of U but this is already away from the heart of finite difference methods. Hence, the convolution with the Gaussian kernel indicated above is a discrete evolution in our case.

If we consider the continuous model, this type of smoothing is equivalent to solving the heat equation

$$\begin{aligned} \partial_t w &= \Delta w \\ w(x,y,0) &= U(x,y), \end{aligned}$$

where pseudo-time and width are connected via

$$T = \frac{1}{2}\delta^2,$$

i.e. the initial value problem for the heat equation is to be solved until pseudo-time $t = T$ is reached. Care has to be taken in order to choose δ. Too large a δ would be overdiffusive while a very small δ would not reduce the high-frequency noise. Since we work on the discrete level the initial value problem for the heat equation is best cast in discrete form

$$\begin{aligned} U^0_{i,j;\delta} &:= U_{i,j} \\ U^{m+1/2}_{i,j;\delta} &= U^m_{i,j;\delta} + \Delta t \frac{U^m_{i+1,j;\delta} - 2U^m_{i,j;\delta} + U^m_{i-1,j;\delta}}{\Delta x^2} \\ U^{m+1}_{i,j;\delta} &= U^{m+1/2}_{i,j;\delta} + \Delta t \frac{U^{m+1/2}_{i,j+1;\delta} - 2U^{m+1/2}_{i,j;\delta} + U^{m+1/2}_{i,j-1;\delta}}{\Delta y^2}, \end{aligned} \tag{3}$$

where iteration along pseudo time is performed until the iteration index m is some m_{stop} corresponding to $T = \delta^2/2$. At the stopping time we set $U_{i,j;\delta} := U^{m_{stop}}_{i,j;\delta}$.

Note that we utilize an explicit splitting scheme which is stable under the CFL condition $\Delta t/\min(\Delta x^2, \Delta y^2) \le 1/2$, see [6]. An implicit discretization would be better behaved but δ is small so that an explicit splitting

is advantageous with respect to computational effort. As an example we show in figure 4 the result of a pre-smoothing with $\delta = 0.02$. In comparison with figure 1 the filtering influence with respect to high frequency modes can be observed. For the sake of comparison we again plot the difference

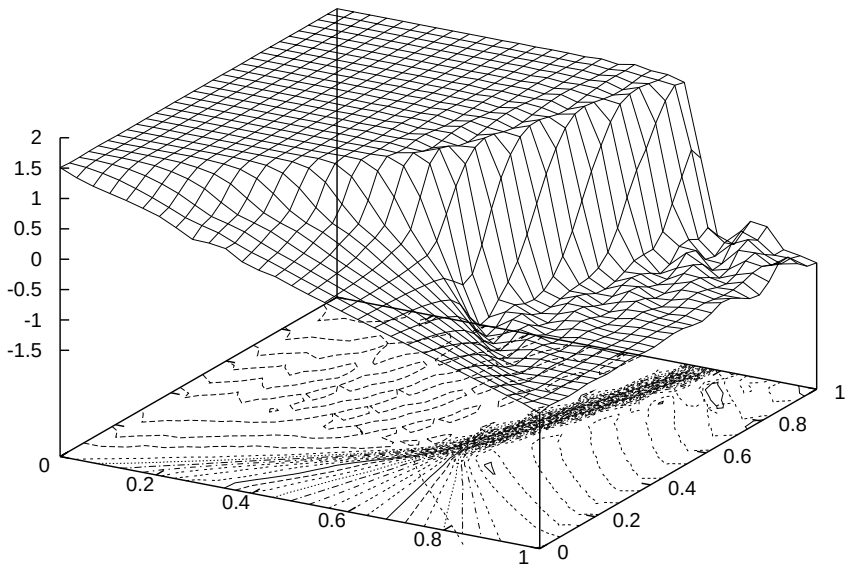

Figure 4: Result after pre-smoothing

between our numerical solution (now after filtering) and the true solution in figure 5. Note that the error is now already concentrated in the vicinity of the shock. However, the application of the linear heat equation seems to be a dangerous step within the overall algorithm. While high-frequency modes are in fact damped the shock structure deteriorates very fast. Thus, it seems wise to start with a nonlinear diffusion equation directly on the unfiltered data and leave the task of filtering completely to this nonlinear device. From the pre-smoothed solution U_δ we compute the structure tensor

$$J_0(\nabla U_{i,j;\delta}) := \nabla U_{i,j;\delta} \cdot \nabla U_{i,j;\delta}^T. \tag{4}$$

Since we are still as discrete as possible the meaning of our operator is

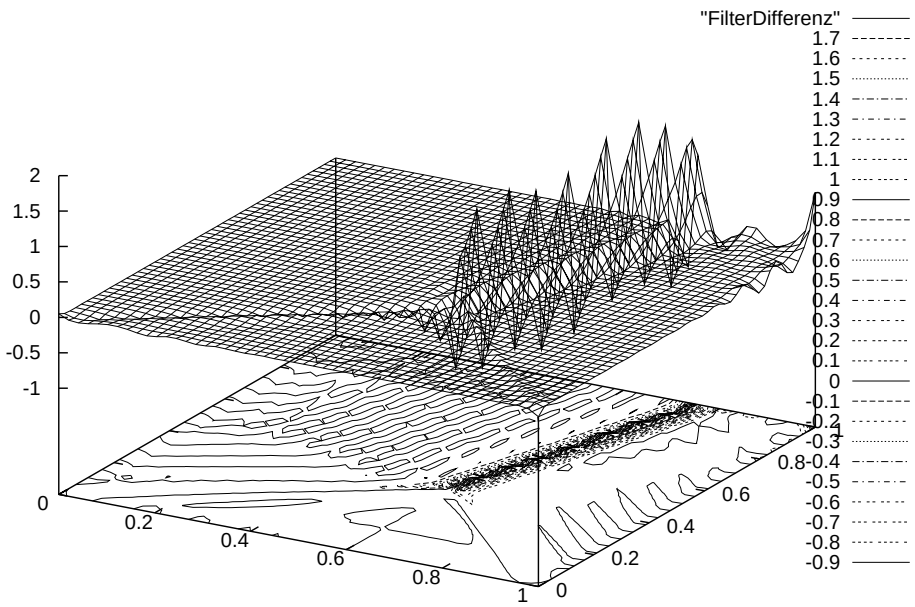

Figure 5: Difference between pre-smoothed solution and true solution

defined as

$$\nabla u_{i,j;\delta} := \begin{pmatrix} \dfrac{u_{i+1,j;\delta} - u_{i-1,j;\delta}}{2\Delta x} \\ \\ \dfrac{u_{i,j+1;\delta} - u_{i,j-1;\delta}}{2\Delta y} \end{pmatrix}. \tag{5}$$

Note that the structure tensor is symmetric positive semidefinite.

An easy calculation reveals the eigenvalues

$$\lambda_1 = |\nabla u_{i,j;\delta}|^2, \quad \lambda_2 = 0$$

corresponding to the eigenvectors

$$v_1 = \nabla u_{i,j;\delta}, \quad v_2 = \nabla^{\perp} u_{i,j;\delta},$$

where

$$\nabla^{\perp} u_{i,j;\delta} := \begin{pmatrix} -\left(\dfrac{u_{i,j+1;\delta} - u_{i,j-1;\delta}}{2\Delta y}\right) \\ \\ \dfrac{u_{i+1,j;\delta} - u_{i-1,j;\delta}}{2\Delta x} \end{pmatrix}$$

so that $\nabla U_{i,j;\delta}^T \cdot \nabla^\perp U_{i,j;\delta} = 0$. In fact, the eigenvectors of the structure tensor define the direction parallel to, and across an edge, respectively. In the framework of image processing the eigenvalues give the contrast (i.e. the squared gradient) in the eigendirections.

Since the structure tensor is symmetric positive semidefinite we have the splitting

$$J_0(\nabla U_{i,j;\delta}) = V \Lambda V^{-1}, \tag{6}$$

where V is the matrix (v_1, v_2) containing the eigenvectors and Λ is nothing but $\mathrm{diag}(\lambda_1, \lambda_2)$.

In order to average the structure tensor data in the vicinity of each grid point component-wise convolution with the Gaussian kernel of width ρ is applied, i.e.

$$J_\rho(\nabla U_{i,j;\delta}) := K_\rho * \left(\nabla U_{i,j;\delta} \cdot \nabla U_{i,j;\delta}^T\right) \tag{7}$$

is computed. The width ρ again is a measure of the averaging region. In practice, we again solve the discrete heat equation component-wise for the structure tensor.

A simple computation concerning the matrix $J_\rho(\nabla U_{i,j;\delta}) =: \begin{pmatrix} j_{11} & j_{12} \\ j_{12} & j_{22} \end{pmatrix}$ reveals the eigenvalues

$$\lambda_{1,2;\rho} = \frac{1}{2}\left(j_{11} + j_{22} \pm \sqrt{(j_{11} - j_{22})^2 + 4j_{12}^2}\right), \tag{8}$$

the positive square root belonging to $\lambda_{1;\rho}$, which correspond to the eigenvectors

$$\begin{aligned} v_{1;\rho} &= \begin{pmatrix} 2j_{12} \\ j_{22} - j_{11} + \sqrt{(j_{11} - j_{22})^2 + 4j_{12}^2} \end{pmatrix} \\ v_{2;\rho} &= \begin{pmatrix} j_{11} - j_{22} - \sqrt{(j_{11} - j_{22})^2 + 4j_{12}^2} \\ 2j_{12} \end{pmatrix} \end{aligned} \tag{9}$$

which are again orthogonal. A nice interpretation of these quantities in the framework of image processing can be found in [12]. The parameter δ in the pre-smoothing processing is called the local scale or noise scale, because the process of pre-smoothing neglects all scales smaller than $\mathcal{O}(\delta)$. In contrast, the parameter ρ is the integration scale indicating the size of the subregions in which the orientation of the numerical solution is analyzed. The eigenvalues $\lambda_{1,2;\rho}$ moreover serve as descriptors of local structure. Constant solutions are characterized by $\lambda_{1;\rho} = \lambda_{2;\rho} = 0$, while the quantity

$$(\lambda_{1;\rho} - \lambda_{2;\rho})^2 = (j_{11} - j_{22})^2 + 4j_{12}^2$$

becomes large for anisotropic structures. In the language of image processing one speaks of $(\lambda_{1;\rho} - \lambda_{2;\rho})^2$ as a measure of local coherence.

Now that we have analyzed our numerical solution as if it was a photograph, we are finally looking for a nonlinear, anisotropic diffusion equation of the form

$$\begin{aligned} \partial_t w &= \text{div } (D(w)\text{grad } w) \\ w(x, y, 0) &= U_\delta(x, y), \end{aligned}$$

where the dissipation coefficient $D(w)$ makes use of the information contained in the structure tensor. It is here where we again use the machinery of image processing since we follow the ansatz

$$D(w) := V_\rho L V_\rho^{-1} \tag{10}$$

where V_ρ contains the eigenvectors of J_ρ and $L = \text{diag}(l_1, l_2)$ is a diagonal matrix the entries of which we have to choose properly. In order to recover shocks (or, equivalently, in order to enhance edges), the diffusivity l_1 perpendicular to edges should be reduced if the contrast $\lambda_{1;\rho}$ is high. This can be achieved by an anisotropic regularization of the famous Perona-Malik model, which again can be found in Weickert's book [12]:

$$\begin{aligned} l_1 &= \vartheta(\lambda_{1;\rho}) \\ l_2 &= 1 \\ \vartheta(s) &= \begin{cases} 1 & ; \quad s \leq 0 \\ 1 - \exp\left(\frac{-C_m}{(s/\lambda)^m}\right) & ; \quad s > 0 \end{cases} \end{aligned} \tag{11}$$

The values of m and C_m are chosen in such a way, that the so-called flux $\Phi(s) := s\vartheta(s)$ is increasing in an interval $s \in [0, \lambda]$ and decreasing in $s \in]\lambda, \infty[$. These choices depend on a one-dimensional analysis of the classical Perona-Malik model and we refer the reader to Weickert's book for details. In agreement with Weickert we chose $m = 4$ and thus $C_4 = 3.31488$. The parameter λ can then be chosen freely.

5 Discretizing the diffusion equation

After deriving a nonlinear anisotropic diffusion equation which will sharpen the shocks this equation needs now to be discretized. Since we do not have a theory of a truely discrete diffusion equation to start with but a partial differential equation the discretization process may result in instabilities if done in a naive way.

As was shown by Weickert [12] there is always a finite difference stencil such that the resulting discretization leads to a stable scheme. Moreover, Weickert was able to prove that three directions suffice to discretize the anisotropic diffusion and the proof is constructive. We do not want to go into the details of Weickert's work but give a suitable discretization of div $(D(w)\text{grad } w)$ where we utilize the notation

$$D = \begin{pmatrix} a & b \\ b & c \end{pmatrix}.$$

Then, following Weickert's recipe, we get

$$\nabla \cdot (D(U_{i,j;\delta})\nabla U_{i,j;\delta}) = \sum_{k=-1}^{1} \sum_{\ell=-1}^{1} C_{i+k,j+\ell} U_{i+k,i+\ell;\delta}$$

with

$$\begin{aligned}
C_{i-1,j+1} &= \frac{|b_{i-1,j+1}| - b_{i-1,j+1}}{4\Delta x\Delta y} + \frac{|b_{i,j}| - b_{i,j}}{4\Delta x\Delta y} \\
C_{i-1,j-1} &= \frac{|b_{i-1,j-1}| + b_{i-1,j-1}}{4\Delta x\Delta y} + \frac{|b_{i,j}| + b_{i,j}}{4\Delta x\Delta y} \\
C_{i,j+1} &= \frac{c_{i,j+1} + c_{i,j}}{2\Delta y^2} - \frac{|b_{i,j+1}| + |b_{i,j}|}{2\Delta x\Delta y} \\
C_{i,j-1} &= \frac{c_{i,j-1} + c_{i,j}}{2\Delta y^2} - \frac{|b_{i,j-1}| + |b_{i,j}|}{2\Delta x\Delta y} \\
C_{i+1,j+1} &= \frac{|b_{i+1,j+1}| + b_{i+1,j+1}}{4\Delta x\Delta y} + \frac{|b_{i,j}| + b_{i,j}}{4\Delta x\Delta y} \\
C_{i+1,j-1} &= \frac{|b_{i+1,j-1}| - b_{i+1,j-1}}{4\Delta x\Delta y} + \frac{|b_{i,j}| - b_{i,j}}{4\Delta x\Delta y} \\
C_{i-1,j} &= \frac{a_{i-1,j} + a_{i,j}}{2\Delta x^2} - \frac{|b_{i-1,j}| + |b_{i,j}|}{2\Delta x\Delta y} \\
C_{i+1,j} &= \frac{a_{i+1,j} + a_{i,j}}{2\Delta x^2} - \frac{|b_{i+1,j}| + |b_{i,j}|}{2\Delta x\Delta y} \\
C_{i,j} &= -\frac{a_{i-1,j} + 2a_{i,j} + a_{i+1,j}}{2\Delta x^2} \\
&\quad -\frac{|b_{i-1,j+1}| - b_{i-1,j+1} + |b_{i+1,j+1}| + b_{i+1,j+1}}{4\Delta x\Delta y} \\
&\quad -\frac{|b_{i-1,j-1}| + b_{i-1,j-1} + |b_{i+1,j-1}| - b_{i+1,j-1}}{4\Delta x\Delta y} \\
&\quad +\frac{|b_{i-1,j}| + |b_{i+1,j}| + |b_{i,j-1}| + |b_{i,j+1}| + 2|b_{i,j}|}{2\Delta x\Delta y}
\end{aligned}$$

$$-\frac{c_{i,j-1} + 2c_{i,j} + c_{i,j+1}}{2\Delta y^2}$$

and employ a simple forward difference in time.

We remark in passing that the approach presented above is fully conservative. This is expressed as the property of conservation of mean grey level in image analysis, see [12].

6 A new splitting scheme

In the foregoing sections we have described in detail how algorithms and methodology established in image processing can be used in the framework of numerical methods for conservation laws. In order to get a true scheme for conservation laws and not just a post-processing tool we consider now the coupling

$$U_{i,j}^{n+1} = \mathcal{D}(\Delta\tau)\mathcal{C}(\Delta t)U_{i,j}^{n}$$

where $\mathcal{C}$ is the operator associated with the convective part (the Lax-Wendroff method in our setting) while $\mathcal{D}$ represents the operator of nonlinear anisotropic diffusion. Note that Δt is the time scale of our convection problem but $\Delta\tau$ is an independent scale for the nonlinear diffusion part. The above splitting is known to be of first order in time only but our considerations also work out for more sophisticated splittings like Strang's. Note that time accuracy in our steady test case is by no means mandatory. The splitting means that in each time step we apply the discrete convection (i.e. the Lax-Wendroff scheme) first and the nonlinear diffusion part afterwards.

Since the pre-smoothing step using the linear heat equation can not be controlled efficiently (the numerical solution deteriorates massively if the smoothing variance is only marginally too high) this algorithmic step was simply left out. The anisotropic nonlinear diffusion equation was weighted with a factor $\Delta x\Delta y$ in order to guarantee consistency, i.e. we compute

$$\begin{aligned} w_{i,j}^{0} &:= \mathcal{C}(\Delta t)U_{i,j}^{n} \\ w_{i,j}^{1} &= w_{i,j}^{0} - \Delta\tau\Delta x\Delta y\nabla\cdot\left(D(w_{i,j}^{0})\nabla w_{i,j}^{0}\right) \\ U_{i,j}^{n+1} &= w_{i,j}^{1}. \end{aligned}$$

Now the dose of dissipation depends on the spatially mesh as it should while the accuracy of the space discretization is retained. Note that in principle we can allow for more than one pseudo time step in the nonlinear diffusion equation. However, since we like to interprete this equation as

an artificial dissipation, one step is natural. Our numerical experiments furthermore indicate that one diffusion step in fact is enough to achieve results with high resolution.

The parameter chosen for the nonlinear diffusion is $\lambda = 10$, $\rho = 2\sqrt{\Delta x}\sqrt{\Delta y}$.

In figure 6 we show the numerical solution of our splitting scheme after 50, 100, and 150 time steps on the left side. On the right the corresponding coherence measure $(\lambda_{1;\rho} - \lambda_{2;\rho})^2$ is plotted in logarithmic scale, where all data were shifted by 1 in order to avoid the computation of the logarithm of zero. One can see that this measure in fact indicates regions of anisotropic phenomena.

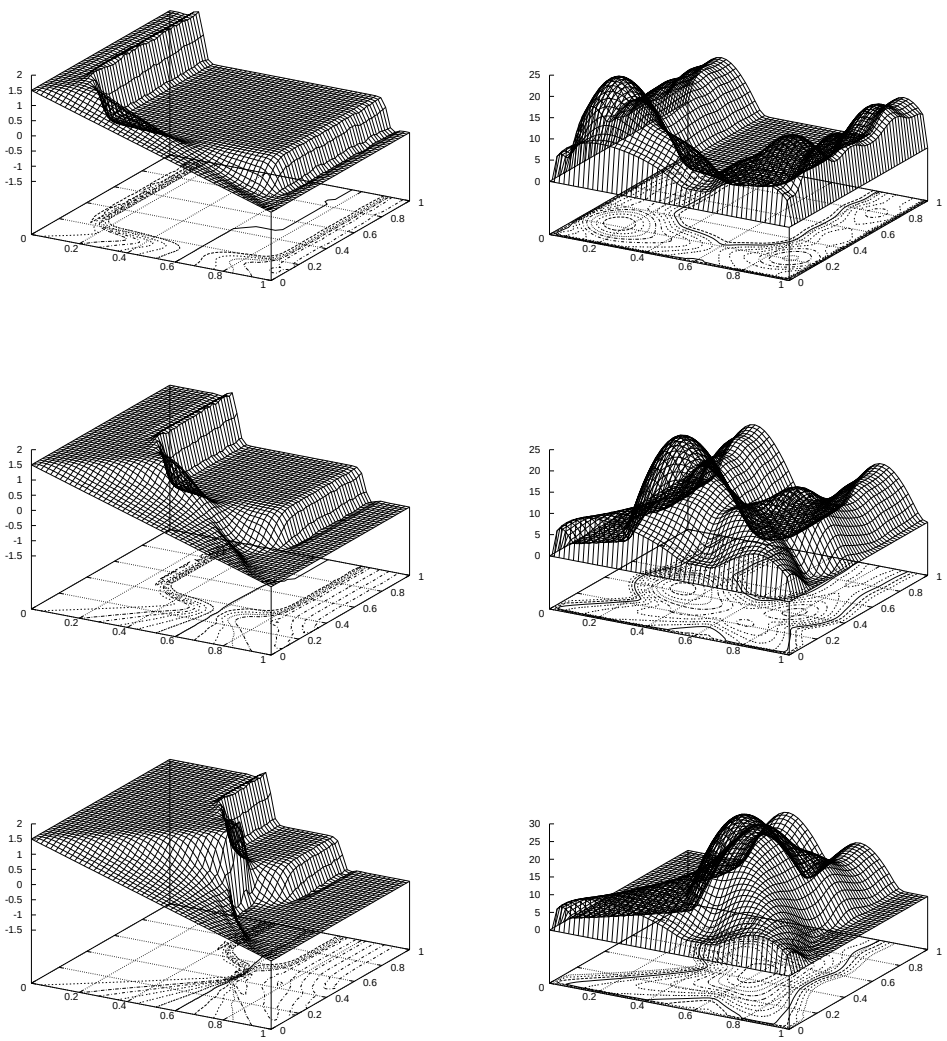

Figure 6: Numerical solution and coherence measure after 50, 100 and 150 time steps

Figure 7 shows the results at later times after 200, 250 and 300 time steps. The shock is now formed and constantly sharpened by the diffusion step.

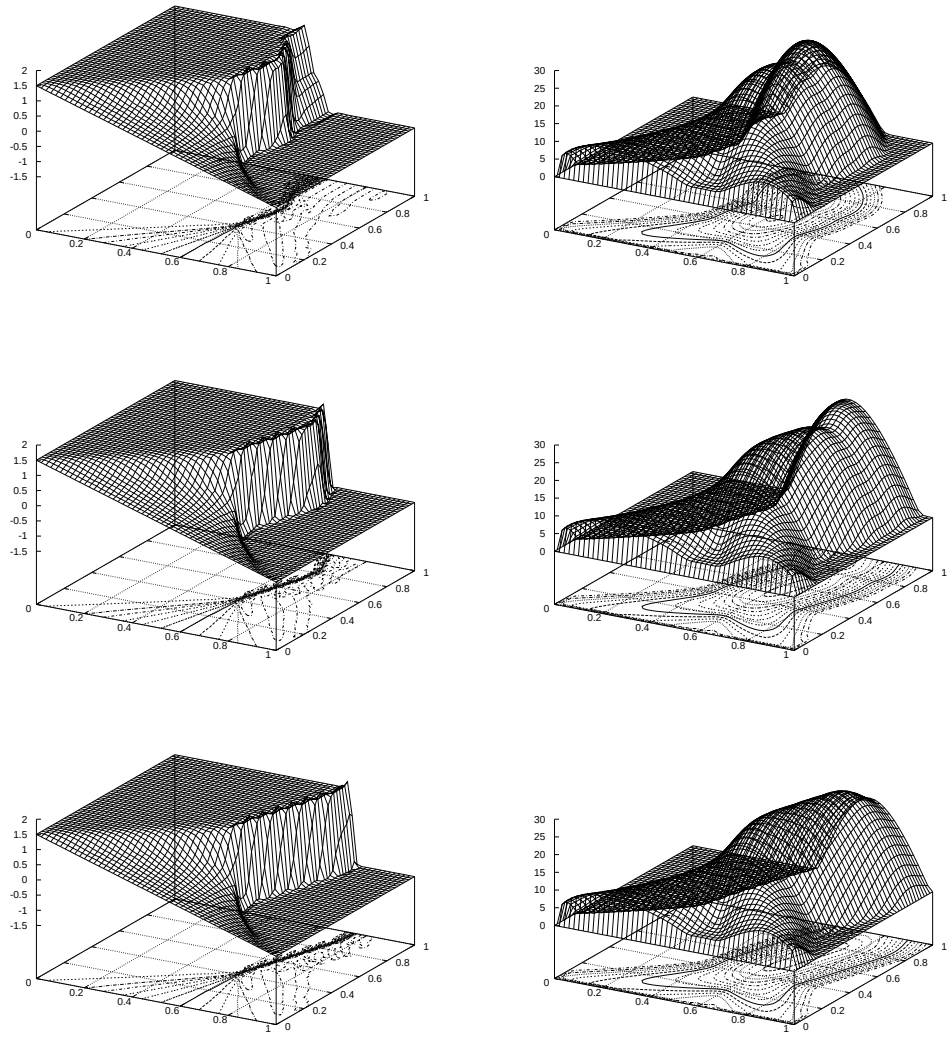

Figure 7: Numerical solution and coherence measure after 200, 250 and 300 time steps

Figure 8 shows the steady state (1000 time steps) and the corresponding coherence measure. Note that the shock is sharply resolved while there are marginal overshoots at the onset of the shock. In contrast to the result of the pure Lax-Wendroff scheme (cp. figure 1) we observe that the splitting scheme with the new anisotropic nonlinear artificial dissipation behaves very nicely. In order to further reduce the small wiggles in the onset of

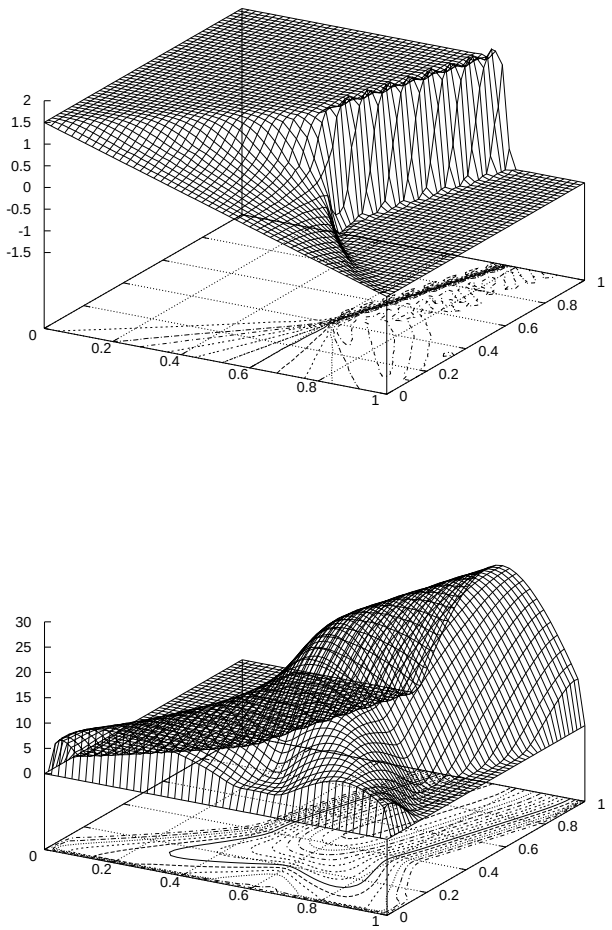

Figure 8: Numerical solution and coherence measure after 1000 time steps (steady state)

the shock the nonlinear diffusion tensor is weighted with the derivatives of the fluxes. This procedure is quite natural if dissipation models of classical finite difference schemes are analyzed, see [7] for example. Instead of

considering the structure tensor $J_\rho(\nabla u) = \begin{pmatrix} j_{11} & j_{12} \\ j_{12} & j_{22} \end{pmatrix}$ we therefore employ

$$\begin{pmatrix} j_{11}(f'(u))^2 & j_{12}f'(u)g'(u) \\ j_{12}f'(u)g'(u) & j_{22}(g'(u))^2 \end{pmatrix}.$$

In figure 9 we show again the numerical solution of our splitting scheme at times $t = 50, 100, 150$.

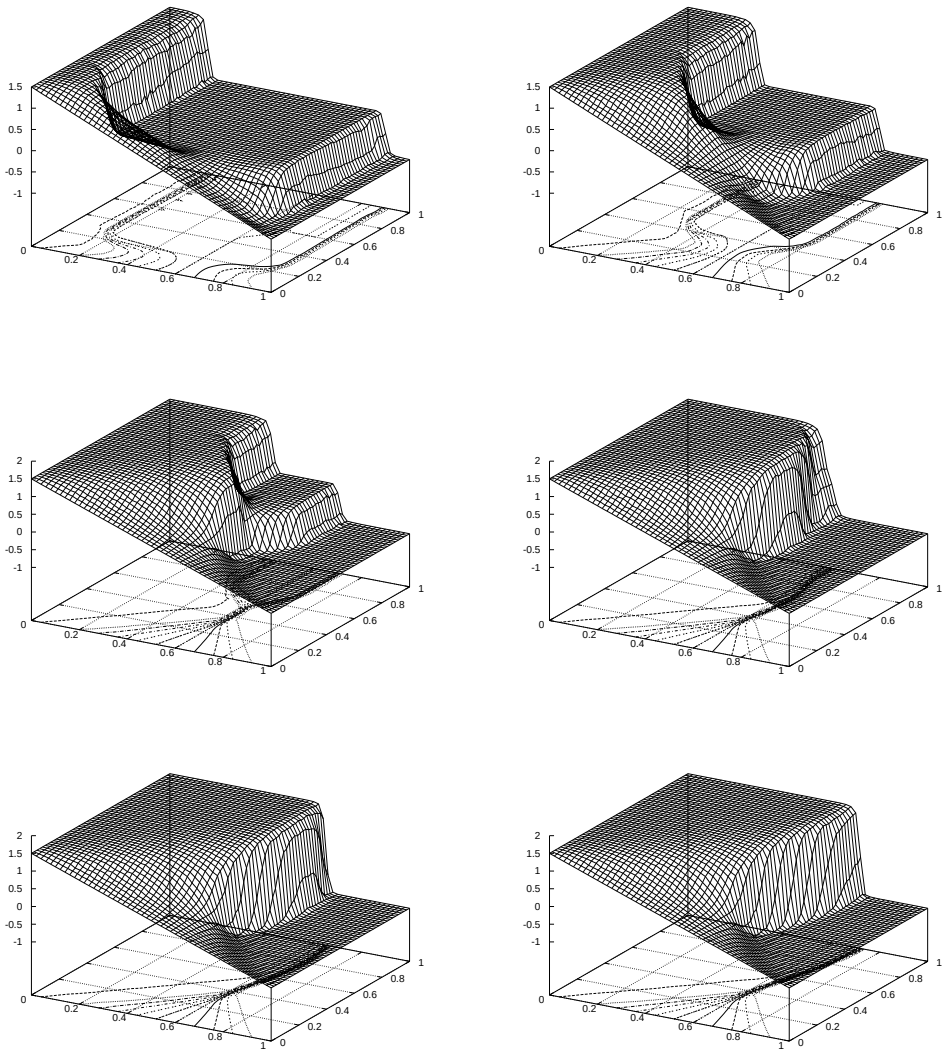

Figure 9: Numerical solution after 50 and 100, 150 and 200, 250 and 300 time steps

Figure 10 shows the steady state. Note that this solution exhibits not only a sharp shock transition but that it is also nearly free of any over- or undershoots. The solution is very close to solutions obtained with modern second-order TVD methods.

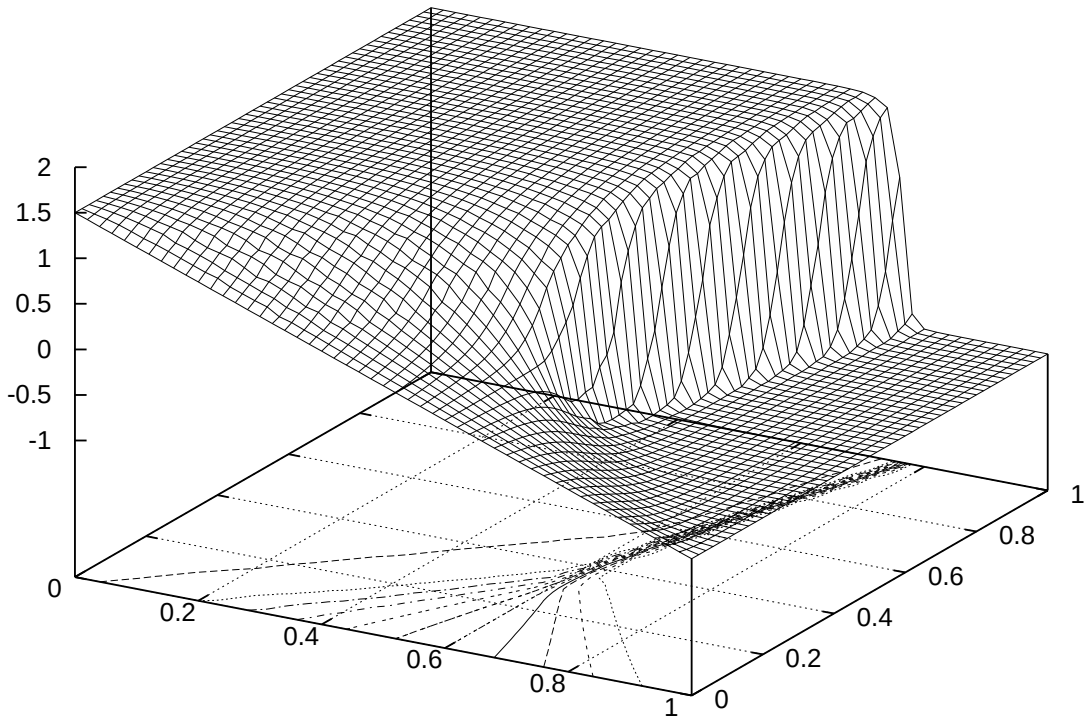

Figure 10: Numerical solution after 1000 time steps (steady state)

Conclusions

We have presented an approach to construct new artificial dissipation terms to be used in the computation of solutions to nonlinear conservation laws. These new dissipation models rely on techniques common in image processing and provide nonlinear and anisotropic artificial dissipation terms. While the construction of classical artificial dissipation is somehow *ad hoc*

the theory of anisotropic diffusion allows dissipation terms build on a sound mathematical footage. The approach is fully conservative because it is entirely based on conservation laws. Moreover, there is now hope to find useful dissipation terms which can be employed in meshless methods, see [1], where up to now higher order discretizations are not achievable.

The class of new schemes constructed as described above have to be further examined concerning their accuracy and stability properties. This mathematical analysis will be the topic of future research.

References

[1] Fürst, J., Sonar, Th. – On meshless collocation approximations of conservation laws: Preliminary investigations on positive schemes and dissipation models. submitted: ZAMM, 1998

[2] Jameson, A., Schmidt, W., Turkel, E. – Numerical Solutions of the Euler Equations by Finite Volume Methods Using Runge Kutta Time Stepping Schemes. AIAA-paper 81-1259, 1981, unpublished

[3] Meister, A., Sonar, Th. – Finite Volume Schemes for Compressible Fluid Flow. in press: Surveys of Mathematics in Industry, 1998

[4] Morel, J.-M., Solimini, S. – Variational Methods in Image Segmentation. Birkhäuser, 1995

[5] Shokin, Yu.I. – The Method of Differential Approximation. Springer Series in Computational Physics, 1983

[6] Sod, G.A. – Numerical Methods in Fluid Dynmaics. Cambridge University Press, 1985

[7] Sonar, Th. – Entropy Production in Second-Order Three-Point Schemes. Numerische Mathematik **62**, 371-390, 1992

[8] Sonar, Th. – Mehrdimensionale ENO-Verfahren. B.G. Teubner, Stuttgart, 1997

[9] Tadmor, E. – The Large-Time Behaviour of the Scalar, Genuinely Nonlinear Lax-Friedrichs Scheme. Math. Comp. **43**, 353-368, 1987

[10] Tadmor, E. – Numerical Viscosity and the Entropy Condition for Conservative Difference Schemes. Math. Comp. **43**, 369-381, 1987

[11] Torre, V., Poggio, T.A. – On Edge Detection. IEEE Transactions on Pattern Analysis and Machine Intelligence, PAMI-8, No.2, 147-163, 1986

[12] Weickert, J. – Anisotropic Diffusion in Image Processing. B.G. Teubner, Stuttgart, 1989